

# Ionospheric climatology and variability from long-term and multiple incoherent scatter radar observations: variability

S.-R. Zhang and J. M. Holt

Haystack Observatory, Massachusetts Institute of Technology, Westford, Massachusetts, USA

Received: 20 March 2007 – Revised: 26 March 2008 – Accepted: 16 April 2008 – Published: 11 June 2008

**Abstract.** Long-term incoherent scatter radar (ISR) observations are used to study ionospheric variability for two midlatitude sites, Millstone Hill and St. Santin. This work is based on our prior efforts which resulted in an empirical model system, ISR Ionospheric Model (ISRIM), of climatology (and now variability) of the ionosphere. We assume that the variability can be expressed in three terms, the background, solar activity and geomagnetic activity components, each of which is a function of local time, season and height. So the background variability is ascribed mostly to the day-to-day variability arising from non solar and geomagnetic activity sources. (1) The background variability shows clear differences between the bottomside and the topside and changes with season. The  $N_e$  variability is low in the bottomside in summer, and high in the topside in winter and spring. The plasma temperature variability increases with height, and reaches a minimum in summer.  $T_i$  variability has a marked maximum in spring; at Millstone Hill it is twice as high as at St. Santin. (2) For enhanced solar activity conditions, the overall variability in  $N_e$  is reduced in the bottomside of the ionosphere and increases in the topside. For  $T_e$ , the solar activity enhancement reduces the variability in seasons of high electron density (winter and equinox) at altitudes of high electron density (near the F2-peak). For  $T_i$ , however, while the variability tends to decrease at Millstone Hill (except for altitudes near 200 km), it increases at St. Santin for altitudes up to 350 km; the solar flux influence on the variability tends to be stronger at St. Santin than at Millstone Hill.

**Keywords.** Ionosphere (Ionosphere-atmosphere interactions; Mid-latitude ionosphere; Modeling and forecasting)

Correspondence to: S.-R. Zhang  
(shunrong@haystack.mit.edu)

## 1 Introduction

Studies of ionospheric climatology and variability have been pursued by many prior workers. Zhang and Holt (2007) (hereafter Paper I) reported on a study based on long-term databases of multiple incoherent scatter radars (ISRs) that resulted in the ISR ionospheric model (ISRIM) system. This system contains two models: (1) the local ISRIM is constructed for each of the seven ISR sites around the world, i.e., Svalbard, Tromsø, Sondrestrom, Millstone Hill, St. Santin, Arecibo and Shigaraki, based on its long-term dataset. (2) The regional climatology, as presented in Paper I for a latitudinal span of 18–70° N in the American sector, is obtained by combining data from sites with similar longitudes. The present paper, however, deals with local variability derived from observations at a specific site using the technique similar to what is described for local climatology in Paper I. We focus on the two mid-latitude locations, Millstone Hill and St. Santin. These ISR sites have very similar geographic but different magnetic latitudes, with Millstone Hill being closer to sub-auroral latitudes.

The ionospheric variability, or the deviation from climatological means, is a pronounced and permanent feature of the ionosphere. It can occur on hourly, daily, seasonal, and solar cycle scales. In particular, during quiet magnetic conditions, the day-to-day variability or the variability on a temporal scale much less than monthly and seasonally may be considered to be related to activity in the lower atmosphere, including acoustic, tidal, and planetary waves, as well as meteorological processes. See Forbes and Zhang (1997), Forbes (2000), Rishbeth and Mendillo (2001), Altadill and Apostolov (2001), Mendillo et al. (2002), Laštovička (2006), Rishbeth (2006) for some recent publications.

Understanding variability in the upper atmosphere from various aspects, such as characterization, physical causes and prediction, remains an outstanding problem. As a first step toward such understanding, this paper is to characterize and

quantify the ionospheric variability in electron density and plasma temperatures at midlatitudes. Many prior publications (see Bradley et al. (2004) and references therein) have pursued the representation of the variability in  $foF2$ ,  $hmF2$ , and MUF. In particular, a simple empirical distribution of the observational data was used to fit to median, upper and lower decile values (see Bradley et al., 2004, and Wilkinson, 2004). It has also been suggested that the upper and lower quartiles be used to avoid the uncertainty in the decile values in the tail of distribution (see Bilitza, 2003, and Radicella, 2003).

As one of the most powerful ground-based instruments for probing the Earth's upper atmosphere, an incoherent scatter radar (ISR) directly measures the ionospheric electron density  $N_e$ , electron and ion temperatures  $T_e$  and  $T_i$ , and line-of-sight ion velocity over a broad height range. Since the development of ISRs in the 1960's, long-term observational data sets have been accumulating for various ISR sites around the world (Zhang et al., 2005). Long-term ISR observations provide an extremely valuable data source for addressing significant aspects of ionospheric climatology and variability. The advantages of using this data lie in the broad height range afforded by the radars and the variety of parameters it produces. The height variation of the ionospheric electron density variability allows for insight into the relative roles that chemistry and dynamical processes may play, and may provide some hints about its origin. Information on the plasma temperature variability, together with that for the electron density, is suggestive of changes in the coupling between the ions, electrons and neutrals. In summary, unlike other studies, this work pays attention to (1) various ionospheric parameters (not just electron density), (2) variations in a large height range (not just the F2-peak), and (3) two mid-latitude sites with similar geographic but different geomagnetic latitudes.

In the following sections, we first describe the technique used to quantify the local ionospheric variability in the ISRIM system with analyses of uncertainty and data distribution. We then present results and discuss the local variability for Millstone Hill and St. Santin. Further discussion and a summary of this research are given in the last section.

## 2 Characterizing ISRIM local variability

### 2.1 Method

The ISRIM local climatology has been fully described in Paper I and is briefly summarized here. We take a two-step approach. First, the data for each ISR site considered are binned by month and local time. We select a number of height nodes and assume a linear change between two neighboring nodes (i.e., piecewise-linear function for height variation) in this first step of data binning. This change is defined by linear coefficients, and they are assumed to be linear in the solar activity index F10.7p and magnetic activity index 3-hourly

$ap$ , where F10.7p is the average between the daily F10.7 and its 81-day average and  $ap$  is for the previous 3 h. These coefficients for F10.7,  $ap$  and constant terms at each height node are determined through a least-square fit for each of the 12 months  $\times$  24 h bins. Then in the second step, they are further represented by a fully analytical basis function with harmonics for seasonal and local time changes, and a cubic B-spline to give twice-differentiable height variations.

F10.7 and  $ap$  are commonly used indices most appropriate for ionospheric and thermospheric modeling. In particular, from an ionospheric modeling study using F10.7, E10.7 and MgII indices based on long-term incoherent scatter radar observations over Millstone Hill, it is indicated that the long-term behavior of the three indices are identical in representing ionospheric variations, regardless of altitude, local time, and season (Zhang and Holt, 2002).  $K_p$  is a quasi-logarithmic index of the 3-hourly range in magnetic activity.  $ap$  index is, however, on a linear scale. It seems to us that  $ap$  may be better suited to describe our linear assumption between the magnetic activity and ionospheric changes.

Our evaluation of the ionospheric variability is based on the difference (residual) between individual measurements and the corresponding climatological average. The average is provided by the ISRIM local climatology, and the measurements are those used for constructing the ISRIM local climatology. Here the ISRIM climatology and data were obtained from a specific site only; the regional ISRIM climatology, which was derived by combining observational data from various ISR sites as well as wide coverage experiments, is not involved. To calculate the ISRIM climatology, F10.7p,  $ap$ , day number of the year, local solar mean time and geodetic height corresponding to the measurement data are used. The difference is squared and goes into the same modeling system as used to produce the ISRIM climatology, i.e., 1) bin data according to local time and month, 2) represent the height variation by a piecewise-linear function, and represent the solar and magnetic dependence using a linear function with F10.7p and  $ap$  terms, i.e.,

$$\mathfrak{N}^2 = \delta_b^2 + c_1 \times f + c_2 \times a \quad (1)$$

where  $f$  is the normalized F10.7p and  $a$  the normalized  $ap$ , and  $c_1$  and  $c_2$  are linear constants), and 3) after the initial step of least squares fitting the linear coefficients, finally express the bin/node coefficients using a 3-D basis function with cubic B-splines and harmonics such that Eq. (1) becomes

$$\sigma^2 = \sigma_b^2 + k_1 \times f + k_2 \times a. \quad (2)$$

Therefore, the ISRIM variability is coherent with ISRIM climatology in terms of the data source and technique used for handling the data; the ISRIM climatology deals with a specific physical parameter, while the ISRIM variability deals with the mean squared difference of a physical parameter from its climatology value. Our results to be discussed include the (absolute) variability,  $\sigma$ , defined as the square root

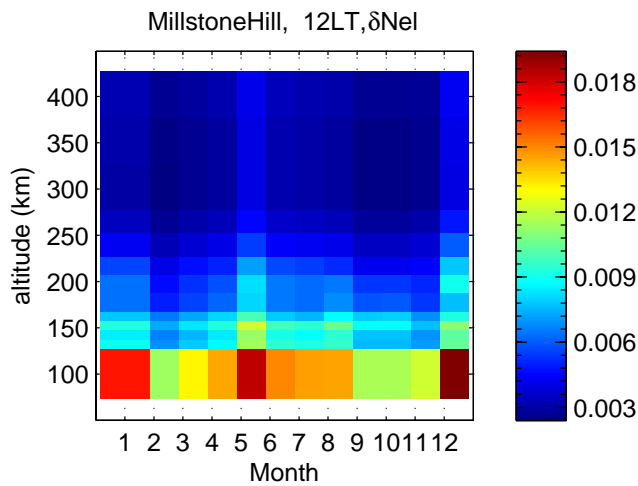


**Fig. 1.** Monthly and height variations of the standard deviation uncertainty in the noon time climatological value of electron density for Millstone Hill.

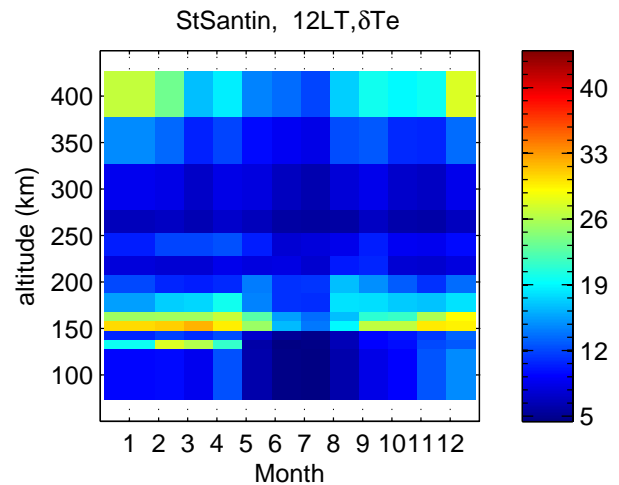


**Fig. 2.** Monthly and height variations of the standard deviation uncertainty in the noon time climatological value of electron temperature for St. Santin.

of the mean squared difference values and the relative or percentage variability defined as the absolute variability divided by the climatology values.

## 2.2 Uncertainty analysis

As in the ISRIM climatology, the ISRIM variability for a given bin is expressed in three terms, a background term, a linear term for solar activity dependency and a linear term for magnetic activity dependence. Any non-linearities will contribute to the background term as second order effects. The background term, varying with different bins with specific local time, month, and height, arises mostly from the day-to-day ionospheric variability that is presumably not linearly associated with solar and magnetic activities. Due to the size of the bins, i.e., 1 h in local time, 3 months in season, and 25–50 km in height (in the region of 200–500 km that we are interested in), the variability within the bin also contributes to our results. Typically, for a given bin there are a few hundreds of data points for St. Santin, and a few thousands of data for Millstone Hill.

We can estimate the ionospheric climatological change within this bin by using the ISRIM climatology. For intermediate solar activity and quiet magnetic activity conditions, at an altitude of 300 km over Millstone Hill,  $N_e$  changes 1–6% within  $12 \pm 0.5$  LT, being smallest in winter. For seasonal trends in 3 months, the  $N_e$  change can be as small as 5% in winter and up to 15–45% in equinox-summer transition periods when  $N_e$  passes through annual maximum and minimum.  $N_e$  changes in height can be somewhat more significant especially near the F2-peak. Therefore, it is important to have an approximate climatological model so that seasonal and altitude changes can be well reproduced. The use of the basis function to represent the variability change with season and

height is also needed to properly interpret variations in the mean squared differences.

As the climatological values are used for the variability estimate, it is worth examining the uncertainty in the climatology values. Now we look at the standard deviation of the fitting that occurs in the first step to obtain bin coefficients in the constant, solar activity and magnetic activity terms (i.e., prior to being loaded into the final fit to the 3-D basis function, see Paper I). Figure 1 shows results of uncertainty in height versus month in the midday  $\log_{10}$  electron density [ $N_{el} = \log_{10}(N_e, \text{m}^{-3})$ ] for Millstone Hill. The uncertainty is rather small, well below 0.1  $\log_{10}(N_e)$  units which is the low limit of the absolute variability of  $N_{el}$  (to be discussed in the next section). The uncertainty is slightly larger below 200 km where relatively less amount of data is available.  $T_e$  is more variable and its correlation with F10.7 and  $ap$  is less evident (Zhang et al., 2005), however, the uncertainty in  $T_e$ , even for St. Santin which has less amount of data available than Millstone Hill, are less than 40°K (Fig. 2), meanwhile, the absolute variability in  $T_e$  (to be discussed below) is normally above 150°K. The uncertainty in  $T_i$  (not shown) has an maximum of 15–20°K, and are about 10–20°K lower than the absolute variability.

Other than that from the climatological values, the uncertainty in the derived variability arises also from binning according to local time, season, and height and from fitting to the three terms. It is found that, for Millstone Hill data, such a uncertainty for midday is estimated as around 0.002–0.01 for  $N_{el}$ , 15–40°K for  $T_e$ , and 5–25°K for  $T_i$ , corresponding to percentages of the background deviation of  $\leq 5\%$  for  $N_{el}$  and  $T_i$  and  $\leq 10\%$  for  $T_e$ . The uncertainty is larger for St. Santin where less observational data are available.

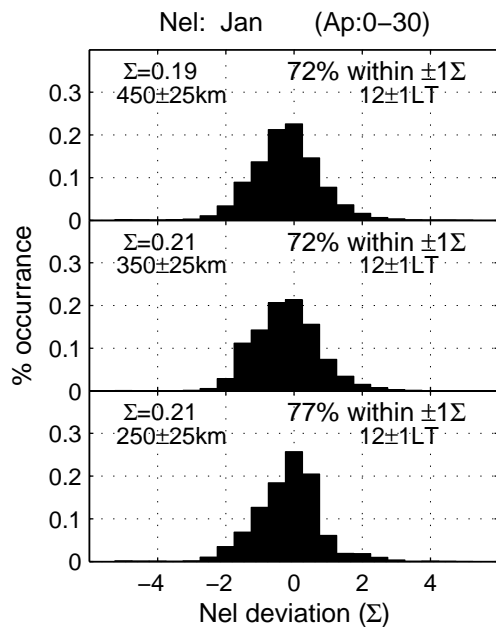


**Fig. 3.** Percentage distribution of the midday deviation from climatological values for electron density in January over Millstone Hill. The horizontal axis is in units of  $\log_{10}(Ne, \text{m}^{-3})$ . Three panels are for three altitudes, i.e., 450 km (top), 350 km (middle) and 250 km (bottom). Also marked in the figure is the total percentage occurrence for the deviation within 1 standard deviation unit.

### 2.3 Distribution

The distribution of the data deviation from climatological values carries important information on the variability. With *ap* in a range of 0–30 but no limitation on F10.7, Fig. 3 gives the quiet time distribution of the *Nel* deviation  $\Delta Nel$  for three altitude ranges around noon in January. The distribution is normalized to the number of occurrence at the mean (climatological) value level. The horizontal axis is in the unit of standard deviation of  $\Delta Nel$ . We see the quiet time standard deviation ( $\Sigma$ ) of  $\Delta Nel$ , arising mostly from solar activity variability, is around 0.20 around noon. The majority of the deviation is within  $2\Sigma$  [ $0.4 \log_{10}(Ne)$  unit]. At lower altitudes, 77% data are within  $\pm 1\Sigma$ , and that percentage decreases at higher altitudes, suggesting a higher degree of data spread. The distribution shape is approximately Gaussian though with longer tails, and at lower altitudes, the distribution is somewhat skewed toward more negative values. This perhaps is a result of the nonlinear dependency of the electron density on the F10.7 index (see Paper I and references therein). The F2-layer electron density tends to increase with F10.7 at a smaller rate for very large F10.7 values as compared to the rate for intermediate and low F10.7 values, therefore, if a linear relationship between *Nel* and F10.7 is assumed, *Nel* may be slightly overestimated for some conditions.

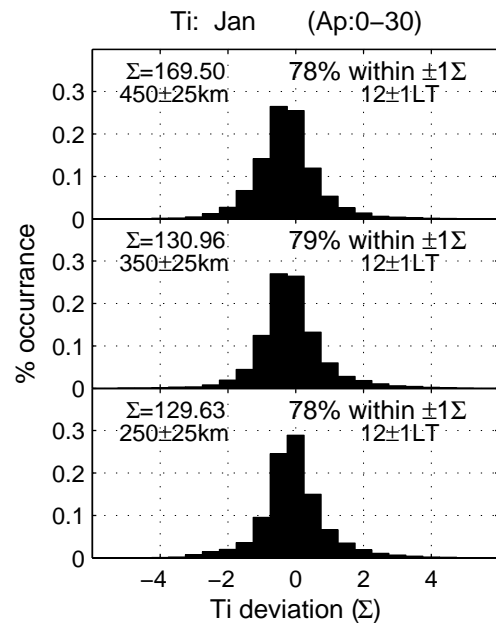


**Fig. 4.** Same as Fig. 3 but for ion temperature.

Ion temperature is more symmetric (Fig. 4). The standard deviation of the deviation  $\Delta Ti$  is between 130–170°K, larger for higher altitudes. However, the percentage occurrence for the deviation within  $\pm 1\Sigma$  is slightly higher than that for  $\Delta Nel$ , and changes little with altitude. The standard deviation of the deviation  $\Delta Te$  is between 215–330°K and increases with height. The percentage occurrence for  $\Delta Te$  within  $\pm 1\Sigma$  is around 70%, less than for  $\Delta Nel$  and  $\Delta Ti$ . The dependency of *Te* on solar activity is a complicated one. At midlatitudes, it is mostly anti-correlated with *Ne* for high solar activity. At low solar activity, however, it tends to be positively correlated to F10.7 (see Zhang and Holt, 2004; Zhang et al., 2004).

### 3 Results: midlatitude variability

Our discussion will focus on midlatitude sites, Millstone Hill and St. Santin. It should be noted that with an invariant latitude of 53°, Millstone Hill is closer to subauroral latitudes that differ from typical midlatitudes in terms of effects of electric fields and particle precipitation under the influence of magnetospheric processes. Variability changes with solar activity, season, local time, and height, however, this paper will not address local time variation but height, seasonal and solar activity variations for the midday. We note that the quality of ISR data and the data availability maximize near midday.

### 3.1 Background variability

As mentioned above, our variability  $\sigma$  for a given time, season and height is expressed in the form of Eq. (2),  $\sigma^2 = \sigma_b^2 + k_1 \times f + k_2 \times a$  where  $k_1$  and  $k_2$  are linear constants and  $\sigma_b$  is the background variability which is presumably independent of solar and magnetic activities (but with possible second order effects from them). We now examine various changes in  $\sigma_b$ . The percentage variability is the absolute variability divided by the ISRIM climatology (i.e.,  $\sigma_b/\text{mean}$ ). These results are shown in Figs. 6–8. From Fig. 6 for  $N_eI$ , we can see following features:

- Variabilities for both sites are similar in the season versus height variation pattern as well as in the magnitude of the variability. The absolute variability  $\sigma_b$  is 0.1–0.2 [or 25–58% in  $N_e$ , estimated based on  $\delta N_e I = \log_{10} N_e - \log_{10} N_{e0} = \log_{10}(N_e/N_{e0})$ ], and the percentage variability ( $\sigma_b/N_eI$ ) is less than 2%; both variabilities are in phase.
- The variability below the F2-peak is lower than above the F2-peak; the variability tends to increase with height within the height range concerned in this study, 200–400 km;
- Clear annual variations of the variability can be identified with high values in spring and winter and low values in summer or earlier autumn. The lowest variability occurs around 225 km in summer.

Variations of the F2-layer electron density at mid-latitudes are controlled by chemical processes and dynamical processes which include contributions of diffusion, winds and electric field induced ion drifts. Photochemical and diffusion processes are associated with neutral atmospheric temperature and composition. These thermospheric changes are slow to settle and they are expected to have a low level of variability during quiet geomagnetic conditions, besides the regular climatological changes in local time, seasonal, and solar cycle, because the temporal and horizontal spatial scales of variations tend to be great (Rishbeth, 1998), so they tend to keep the ionospheric electron density stable. Photoionization is strongest in the F1-region, and it decreases dramatically with height; the ions are recombined and lost in a time constant of about 30 min for around 250 km, and 60 min for 270–290 km at intermediate solar activity. Effects of dynamical processes for time scales shorter than this can be manifested, but longer time scale fluctuations are largely masked by the photochemical-diffusion determined variations.

In the topside, since the photochemical time constant is significantly long and the plasma diffusion time constant is significantly short, the electron density is controlled, to a large extent, by diffusion where the plasma scale height plays an important role. Any small fluctuations near the F2-peak can grow rapidly at the topside which is a few scale

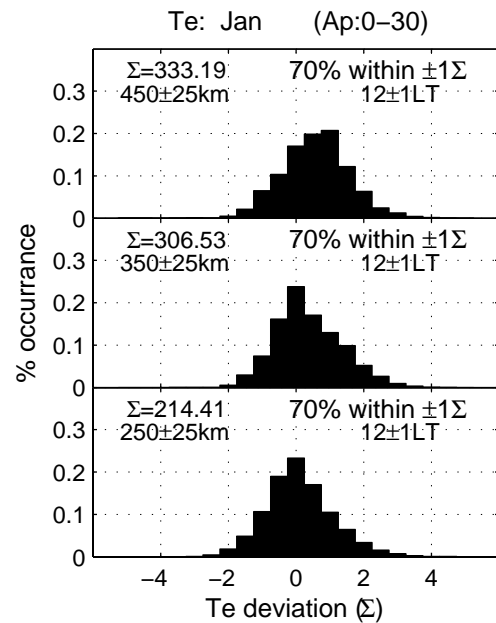


Fig. 5. Same as Fig. 3 but for electron temperature.

heights above the F2-peak. In summary, at low altitudes where photochemical influences are stronger and the day-to-day thermospheric temperature and composition are less variable, the variability is low; at high altitudes where scale height effects are significant, the variability is high.

There are also clear seasonal variations in the variability. It is relatively high in equinox seasons probably because of the summer-winter transition of the thermosphere (Rishbeth and Mendillo, 2001). It is also noted that the photochemical time constant in summer is much shorter than in winter so it takes much less time for the ions in the bottomside to reach their chemical balance.

Figure 7 shows the variability for  $T_e$ . We can see that the variability at both sites is around 150–400°K for  $\sigma_b$ , or 5–20% for  $\sigma_b/T_e$ . It increases markedly with height, especially in the topside. At Millstone Hill, the absolute and relative variabilities peak in spring and autumn, and minimize in summer. At St. Santin, the seasonal peaks in equinox do not show up, rather, there is a single minimum in the summer-autumn period. In the bottomside, the variability tends to be smaller than in the topside over the entire year. A marked minimum appears to be formed in the percentage variability  $\sigma_b/T_e$  at 250 km or slightly below it in summer for the two sites.

Figure 8 shows corresponding results for  $T_i$ . Variability patterns in the absolute value and in the percentage are similar. At Millstone Hill, the variability is around 110–180°K or 10–20%. It tends to be highest around 200 km and lowest around 250 km, and increases above 250 km. It also exhibits peaks in equinox and a minimum in summer. As is well known, at about 220 km and below the ions and neutrals are

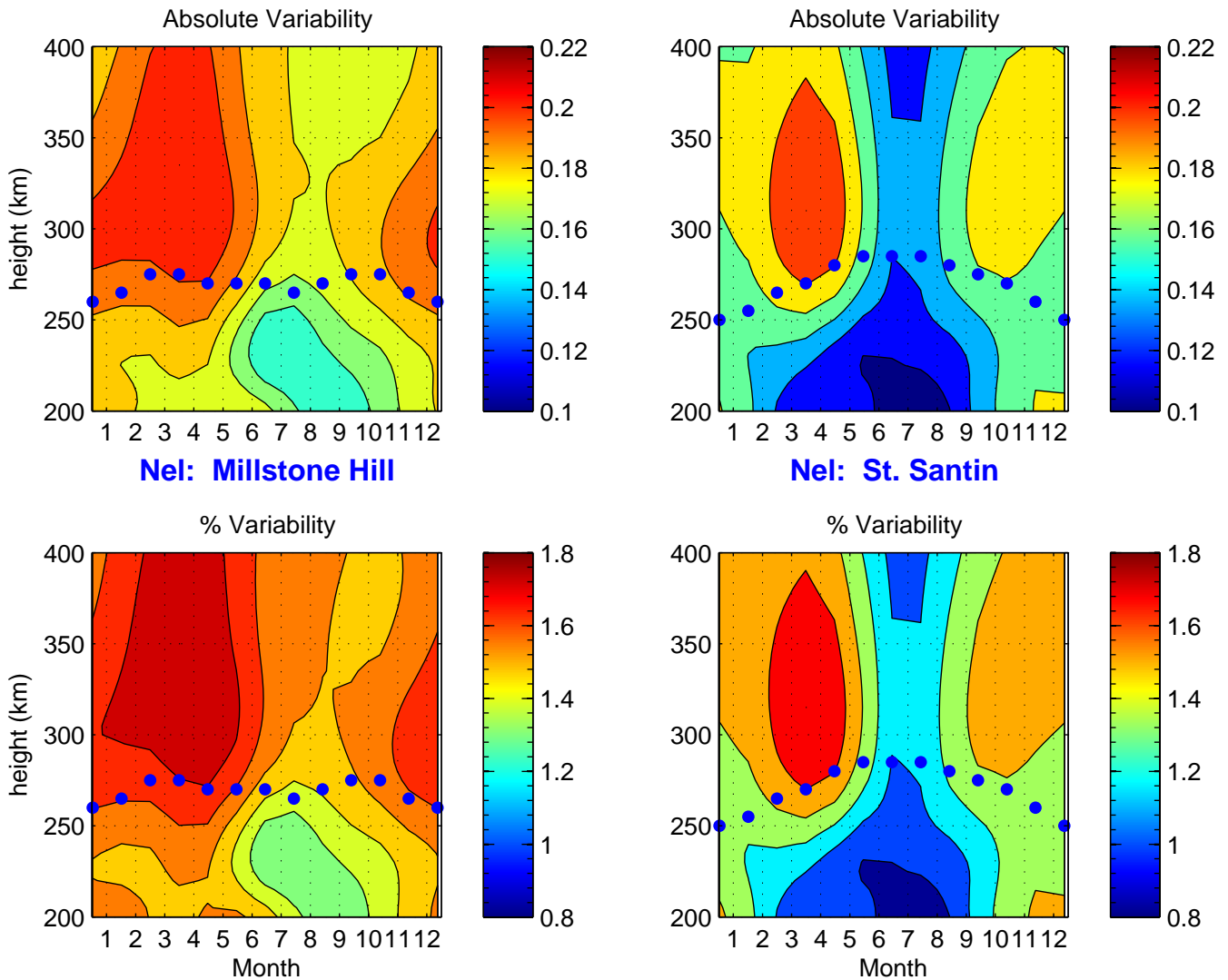


**Fig. 6.** Height and annual variations of the midday absolute and percentage variability for  $Nel$  ( $\sigma_b$  and  $\sigma_b/Nel$ ) at Millstone Hill (left) and St. Santin (right). The percentage variability  $\sigma_b/Nel$  is defined as the absolute variability divided by the ISRIM climatological value. Dots give the height of the F2-peak determined by the ISRIM climatology.

in close thermal contact such that  $T_i$  approximates  $T_n$ ; around 250 km  $T_i$  may be close to the exosphere temperature. Therefore, the ion temperature variability below 250 km should be very close to the neutral temperature variability, which is low for a mid-latitude site.

At St. Santin, however, variabilities are different from those at Millstone Hill, except for the common feature of the summertime minimum in the seasonal variation. The absolute and the relative variabilities in  $T_i$  ( $\sigma_b$  and  $\sigma_b/T_i$ ) are only one half Millstone Hill values. They are not particularly high at lowest heights compared to Millstone Hill. Instead, there exist a striking spring maximum and a summer minimum from 200–400 km. The minimum variability at 250 km shown at Millstone Hill tends to be less clear, especially, in spring.

Some of the differences in the ion temperature variability between the two sites may be explained in terms of differences in magnetic latitudes. Ion temperature variability tends to increase with geomagnetic latitudes from mid-, subauroral to auroral latitudes. At Millstone Hill, for example, the friction heating due to ion-neutral collision can become large for conditions of high ion drifts/electric fields as a result of the auroral zone expansion or electric field penetration. Certain types of particle precipitation may take place as well to give rise to the enhanced ion temperature. These extra heating is more significant at low altitudes from the low F-region through the E-region. The higher background variability at 200 km for Millstone Hill may be resulted from these heating activities.

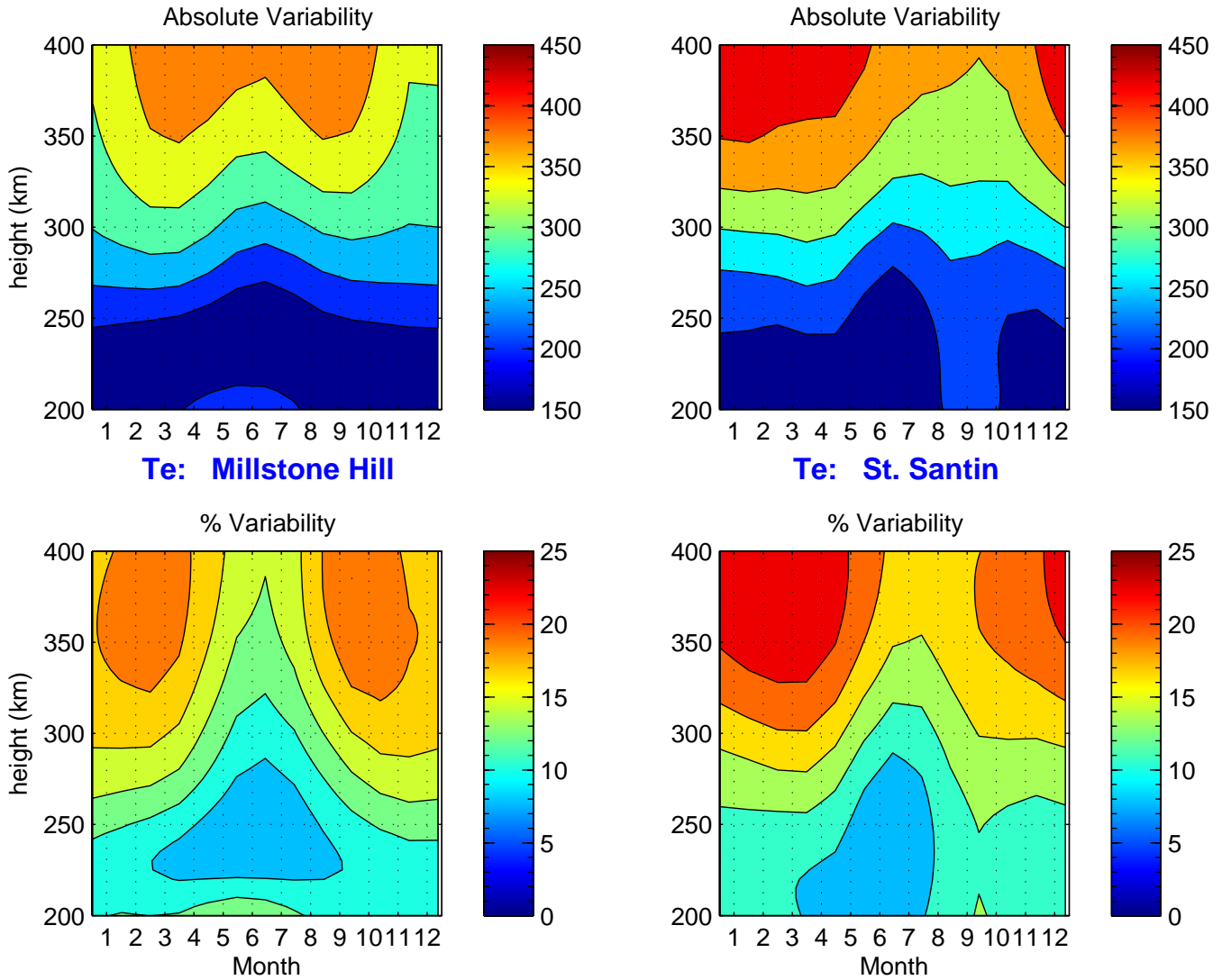


Fig. 7. Same as Fig. 6 but for  $T_e$ .

### 3.2 Solar activity induced variability

Next, we discuss effects of solar activity on the variability. Increased solar flux gives rise to enhanced photoionization, which normally has a maximum in the F1-region, and enhanced heating by photoelectrons. This also produces changes in the neutral atmosphere temperature and composition, therefore causing ionospheric effects. We now examine results of changing F10.7 by 50 units ( $\delta F10.7=50$ ) from 135 (intermediate) to 185 (high) solar activity conditions. This is the F10.7 term in the variability formula (2),  $k_1 \times f$ . Note that, according to our definition,  $k_1 \times f$  can be either positive or negative.

Figure 9 compares the relative change of climatological values with that of the variability. The relative change in the variability [ $\delta(k_1 f)/\sigma_b$ ] is the percentage of the change  $\delta(k_1 f)$  over the background variability  $\sigma_b$  as discussed

above. The relative change in the climatology  $\delta C/C_b$  is the percentage of climatological change  $\delta C$  over the background climatology  $C_b$  (The ISRIM climatology is also expressed in three terms: background, solar and magnetic activity components, in a similar fashion as in the ISRIM variability). As a result of F10.7 increasing by 50 units, the climatological  $Nel$  change increases with height for the two sites. In summer, the response is minimum at Millstone Hill. Since the annual minimum of  $Nel$  background climatological variation  $Nel_b$  is in summer, the absolute climatological change  $\delta Nel$  in summer should be minimum to make the percentage  $\delta Nel/Nel_b$  minimum. These  $Nel_b$  and  $\delta Nel$  minima are due to the effect of low  $O/N_2$  which gives rise to the low F2-peak density, leading to low electron density in the entire F-region as a result of diffusion. The somewhat different seasonal pattern for St. Santin is probably because of the difference in the  $O/N_2$

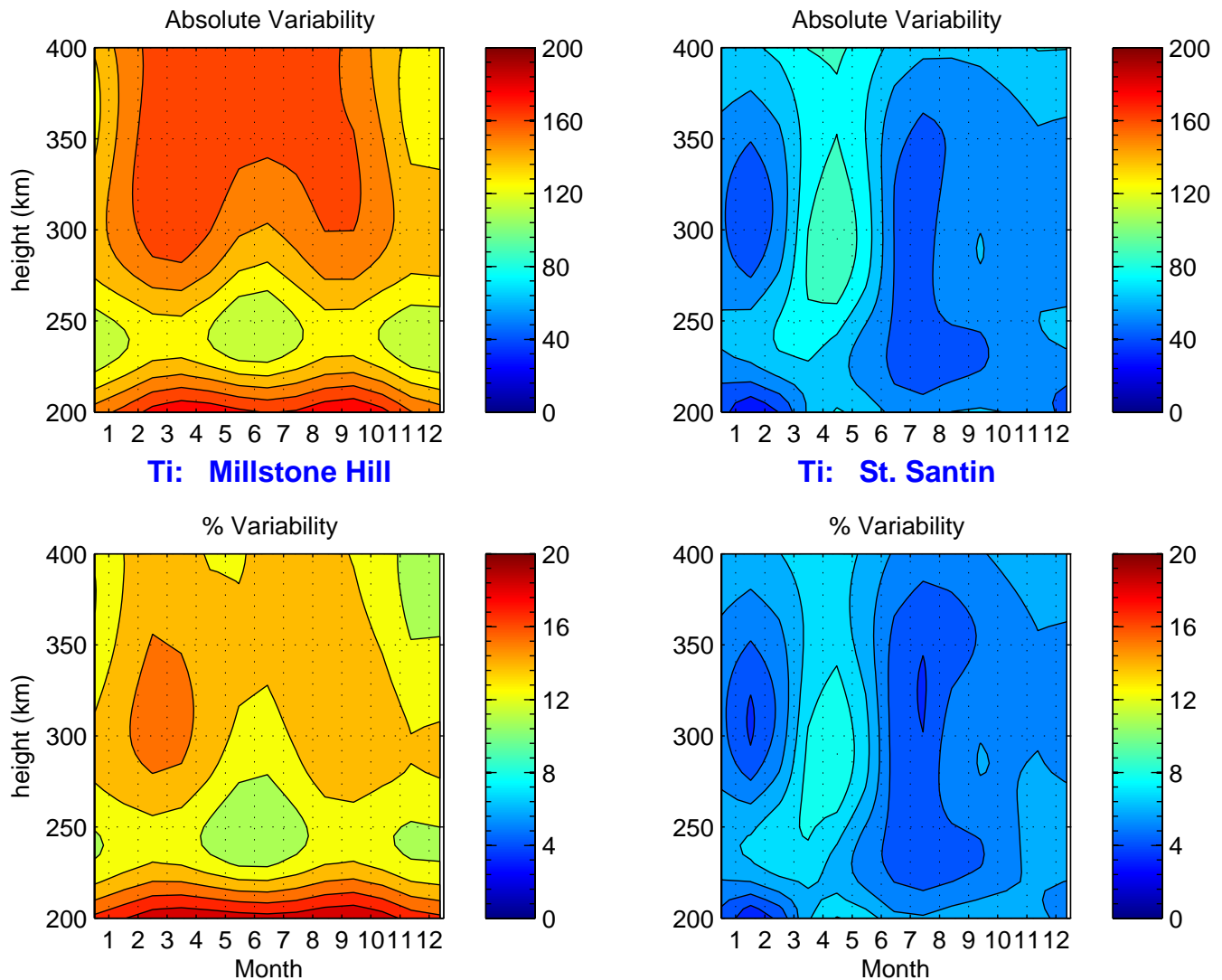


**Fig. 8.** Same as Fig. 6 but for  $T_i$ .

effect which is longitudinally dependent (Rishbeth, 1998). Nevertheless, when the solar activity turns from intermediate to high, the change of  $NeI$  is normally  $\leq 4\%$ . This may be within 10% for changes from solar minimum to maximum.

Changes of the variability  $\delta(k_1 f)/\sigma_b$  responding to the F10.7 increase are very different. Although the climatological change is less than 4%, the variability change can be comparable with the background variability. Below the F2-peak, especially in summer, the variability is negative (reduced); above the peak, the variability is positive (enhanced); near the peak, the percentage change of the variability is little. It is very interesting to note that for below the F2-peak, especially, around 230 km, the background variability is nearly cancelled at high solar activity so that the overall variability is very small.

Figure 10 provides results arranged in the same fashion as in Fig. 9 but for electron temperature. An enhanced solar

flux gives rise to more photoelectrons which heat the ambient electrons and ions at a rate proportional to the plasma density; meanwhile, the increased electron density due to the enhanced solar flux leads to an enhanced electron cooling rate through Coulomb collisions which is proportional to  $Ne^2$ . The actual response of  $Te$  to a change in the solar flux is a result of these two competing processes, in addition to effects of heat conduction at high altitudes, and also depends on the level of background  $Ne$ . The climatological result at Millstone Hill is mostly a negative response of  $Te$  to the F10.7 increase ( $\delta F10.7=50$ ), except for summer when background  $Ne$  is low and  $Te$  increases. At low altitudes,  $Te$  increases with F10.7 due to the strong influence of the neutral temperature. The variability  $\delta(k_1 f)$ , however, tends to be negative to decrease the overall variability in general as a result of the F10.7 enhancement (positive only at high altitudes in summer). At Millstone Hill, the largest decrease appears

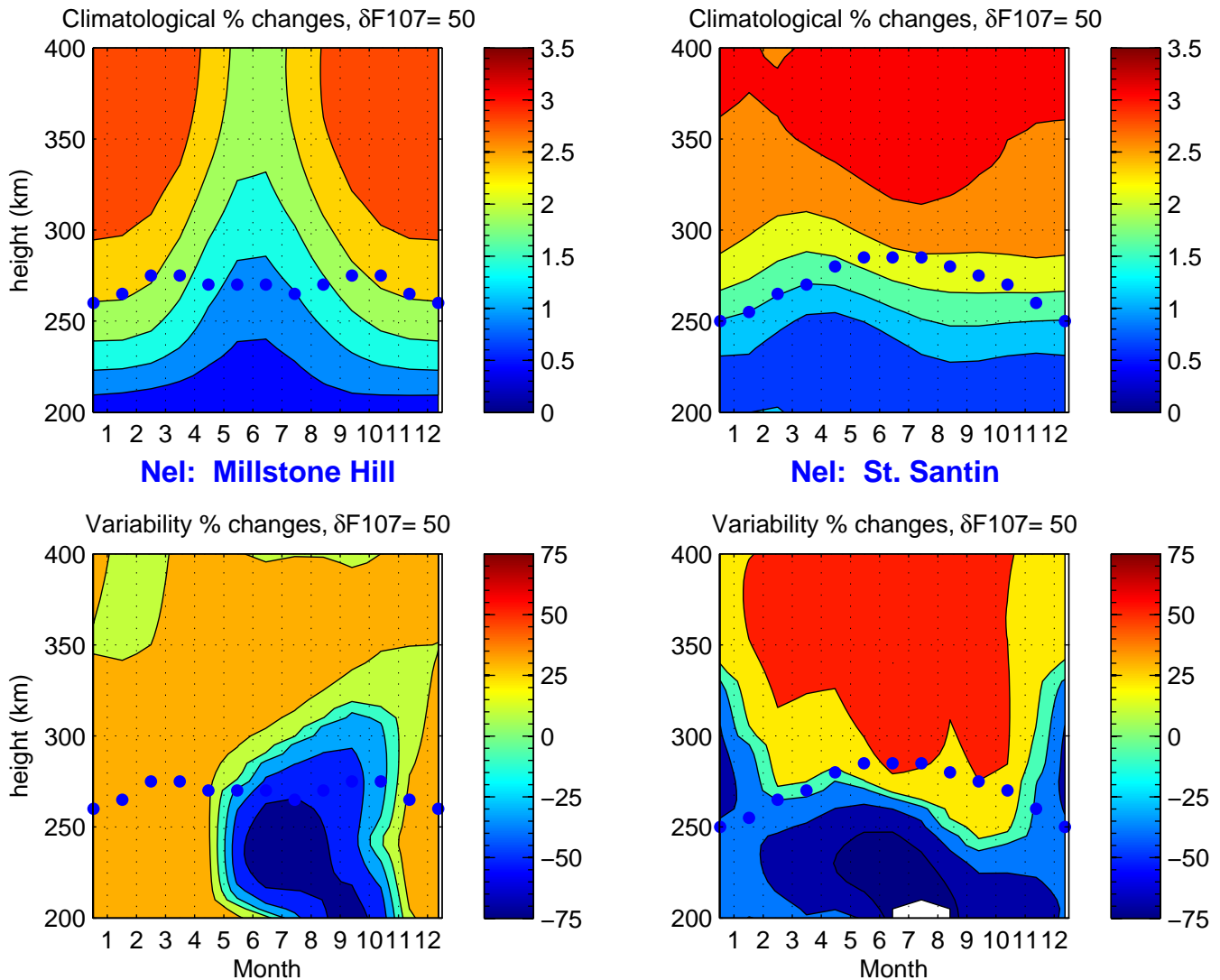


**Fig. 9.** Height and annual variations of F10.7 index effects on the ISRIM climatology (upper panels) and variability (bottom panels) for the midday *NeI* at Millstone Hill (left) and St. Santin (right). The climatological results are percentage changes due to an F10.7 increase of 50 units. The variability results are changes of the variability divided by the background variability. Negative change of the variability indicates the decrease of the variability. Dots give the height of the F2-peak determined by the ISRIM climatology.

to be around 250 km in summer, corresponding to that in *Ne* but with a lower altitude as shown in Fig. 9. At St. Santin, the variability weakens near the F2-peak height. Therefore, near the F2-peak, the variability is small. In general the  $T_e$  variability tends to decrease for conditions of high electron density (near the F2-peak or in winter and equinox), and increase for conditions of low electron density (in the topside or in summer).

Ion temperature normally has a simple linear correlation with the solar activity. The ions are heated by ambient electrons and cooled by neutrals. As shown in Fig. 11, the percentage change in the climatology value over the climatological background as a result of the F10.7 increase by 50 units is

generally uniform in its annual variation, being 10–20%, and is high around 275–350 km. The change of the variability  $\delta(k_1 f)/\sigma_b$  as a result of the F10.7 increase is largely negative for Millstone Hill, indicating the solar activity induced variability cancels the background variability to give the reduced overall variability. There is a slight increase in  $\delta(k_1 f)/\sigma_b$  in autumn; below 230 km, it is large in autumn. The variability in St. Santin exhibits a different behavior from Millstone Hill: the percentage change  $\delta(k_1 f)/\sigma_b$  is much larger, being over 80%. This is due to the larger values of  $\delta(k_1 f)$  (3–4 times the Millstone Hill values; figures not shown) and the smaller background variability  $\sigma_b$  (see Fig. 8), such that the two types of variability are comparable. Furthermore,

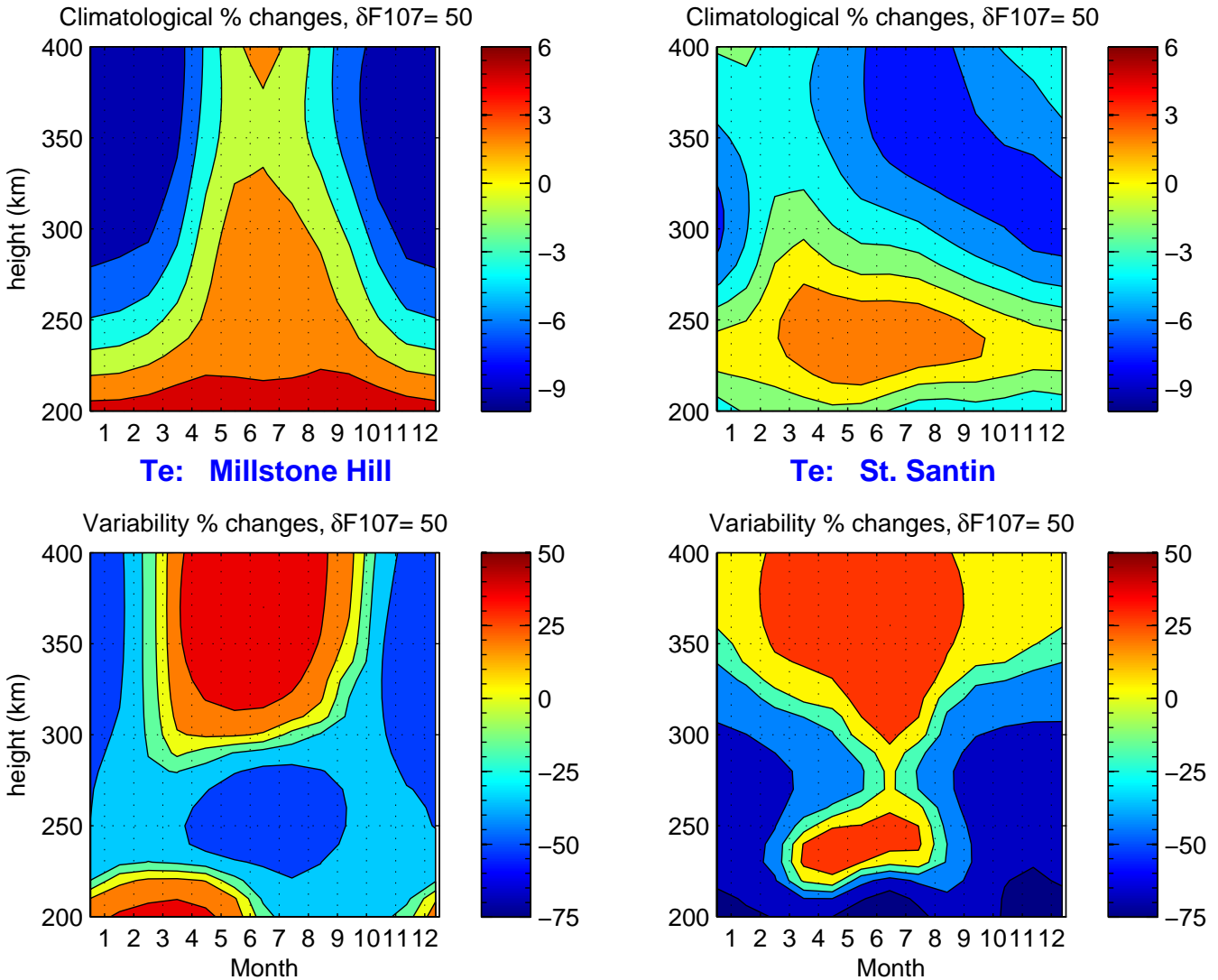


**Fig. 10.** Same as Fig. 9 but for  $T_e$ .

in the broad height range up to 350 km, the solar flux induced variability increases, adding to the overall ion temperature variability. It seems that at Millstone Hill, the background variability is larger and the effects due to solar flux changes are more likely secondary. At St. Santin, the solar flux induced change enhances the overall variability and is very much comparable with the background one. In other words, the St. Santin  $T_i$  variability experiences stronger solar flux influence while the Millstone Hill  $T_i$  variability is largely caused by the background variability, which includes all those not directly dependent of solar and magnetic activities as the first order effect.

This difference in the relative contribution of solar activity effects to the overall variability in  $T_i$  may be also associated with the difference in electron density between the two sites. This is in addition to possible extra heating sources at subauroral latitudes which enter into the background variability as

mentioned earlier. The upper panels of Fig. 11 indicates very similar responses of the  $T_i$  climatology to the F10.7 increase, not only in the general pattern but also in the quantitative sense. This is largely a result of the energy balance for the ions interacting with neutrals and electrons; in the F-region, in particular in the bottomside of the ionosphere,  $T_i$  follows  $T_n$  closely. In terms of variability, however, it is much larger in  $T_e$  than in  $T_n$ , so variability in  $T_e$  contributes significantly to that in  $T_i$ . In fact, the efficiency of electron heating effects, which is proportional to  $Ne^2$ , depends strongly on the level of electron density.  $Ne$  is lower at Millstone Hill than at St. Santin during most months of the year (Zhang et al., 2004), and this difference increases with solar activity. Therefore,  $T_i$  is generally less sensitive to variability in  $T_e$  at Millstone Hill than at St. Santin, and this situation is more evident under high solar activity conditions.

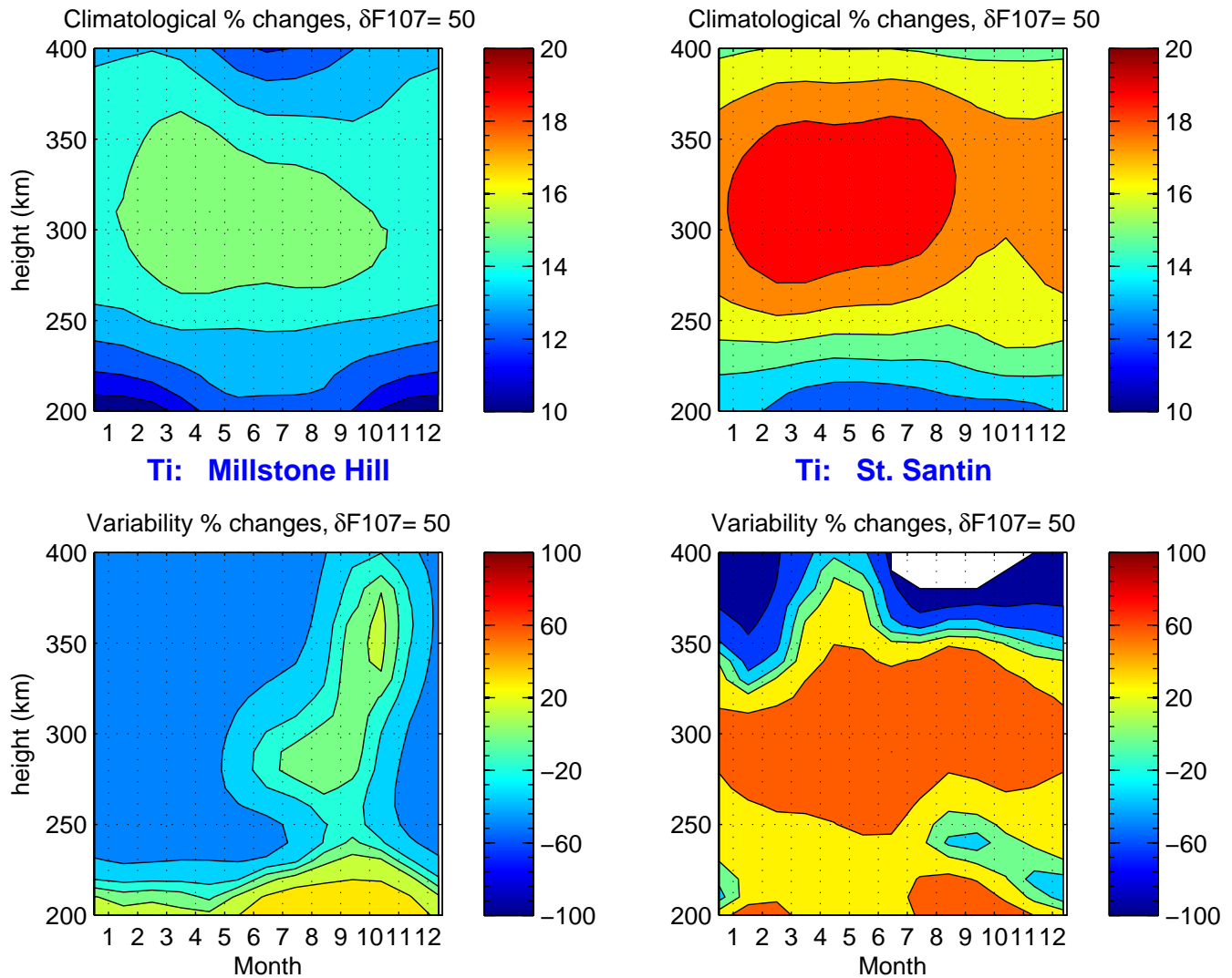


**Fig. 11.** Same as Fig. 9 but for  $T_i$ .

#### 4 Discussion and summary

Ionospheric climatology and variability studies are conducted using long-term incoherent scatter radar (ISR) observations from 7 sites around the world. These studies result in an empirical model system, ISR Ionospheric Model (ISRIM), which describes local and regional ionospheric climatology and variability of the ionosphere.

This paper deals with the ionospheric variability in electron density, ion and electron temperatures at midlatitudes (Millstone Hill and St. Santin). The variability is defined as the deviation between data and ISRIM climatological values, or specifically, the square root of the mean squared data-model difference. It is assumed that the squared difference can be expressed in terms of background, solar activity and magnetic activity contributions, each of which is local time, season and height dependent. We have discussed results of

the background variability and the solar activity induced variability.

Our discussions are not directly associated with effects due to magnetic activity. Due to the relatively simple approach of representing magnetic activity effects, quantifying these effects is still a complicated and challenging issue, and we can not totally rule out their possible contamination of our results. It should be noted, however, the majority of our data, especially, for St. Santin, are from low and intermediate magnetic activities, and it seems unlikely that our results are seriously biased. Seasonal variations of the variability shown in studies on the maximum electron density  $N_{\max}$  by Rishbeth and Mendillo (2001) revealed, for subauroral sites, a weak annual variation with greater variability in winter than in summer, however, being masked by the double peaks in spring and autumn. The double peaks are obviously related to the magnetic activity, since they included data from both

quiet and activity conditions. Their seasonal variability results are for daytime hours between 10:00–16:00 LT, therefore with large contributions from the local time change induced variability. They found no significant correspondence between the quiet day  $N_{\max}$  seasonal pattern and the variability. Our “background” variability for 12:00 LT shows clear annual variability that extends in a broad range of the F2-layer, and corresponds well with the electron density climatology for the annual variation.

We have taken a different approach to measure the ionospheric variability from Forbes (2000) who analyzed  $N_{\max}$  data to quantify various scales of the variability. They calculated mean  $N_{\max}$  values from linear regression with annual, semiannual, solar cycle and daily F10.7 terms (corresponding to our ISRIM climatology), and residuals from the mean determined with various number of regression terms are derived to demonstrate the relative importance of different source of variability. In our results, the background variability is presumed to be non solar activity and magnetic activity origin, such as meteorological processes. It is interesting to note that the variability of ionospheric parameters at Millstone Hill is reduced in the bottomside with increasing solar activity. Since we are not using daily F10.7 index but a compound one, F10.7p, with both short-term (daily) and long-term (3 month) contributions, the daily F10.7 induced variability are not fully considered, but this might be small. Both the case study by Rishbeth (1993) and the statistical study by Forbes (2000) revealed only a weak correlation between the  $N_{\max}$  variability and the day-to-day variability in the solar 10.7 cm flux.

In summary, our study indicates that the background variability shows clear differences between the bottomside and the topside and changes with season. In  $Ne$ , the variability appears to be low in the bottomside in summer, and high in the topside in winter and spring. In plasma temperatures, it increases with height, and reaches a minimum in summer.  $Ti$  variability has a marked maximum in spring; at Millstone Hill it is twice as high as at St. Santin. Examining the solar cycle effect, we find that for enhanced solar activity conditions, the variability in  $Ne$  is reduced in the bottomside of the ionosphere, and increased in the topside. For  $Te$ , the solar activity enhancement reduces the variability in seasons of high electron density (winter and equinox) at heights of high electron density (near the F2-peak). For  $Ti$ , however, while the variability tends to decrease at Millstone Hill (except for altitudes near 200 km), it increases at St. Santin with a high percentage for altitudes up to 350 km; the solar flux influence on the variability tends to be stronger at St. Santin than at Millstone Hill.

*Acknowledgements.* We thank the members of the Haystack Observatory Atmospheric Sciences Group for assembling and maintaining the Madrigal Database. This research was supported by NSF Space Weather Grant ATM-0207748. Observations and researches at Millstone Hill are supported by a cooperative agreement between the National Science Foundation and the Massachusetts Institute of Technology. St. Santin data are imported from the CEDAR database.

Topical Editor M. Pinnock thanks one anonymous referee for her/his help in evaluating this paper.

## References

- Altadill, D. and Apostolov, E. M.: Vertical propagating signatures of wave-type oscillations (2- and 6.5-days) in the ionosphere obtained from electron-density profiles, *J. Atmos. Sol. Terr. Phys.*, 63, 823–834, 2001.
- Bilitza, D.: International Reference Ionosphere (IRI) Task Force Activity 2002 – Chairman’s Report, in: Proceedings of the IRI Task Force Activity 2002, edited by: Radicella, S. M., Report IC/IR/2003/3, Abdus Salam International Centre for Theoretical Physics, Trieste, 2003.
- Bradley, P. A., Kouris, S. S., Stanislawski, I., Fotiadis, D. N., and Juchnikowski, G.: Day-to-day variability of the IRI electron density height profile, *Adv. Space Res.*, 34, 1869–1877, doi:10.1016/j.asr.2004.05.003, 2004.
- Forbes, J. M., Palo, S. E., and Zhang, X.: Variability of the ionosphere, *J. Atmos. Sol. Terr. Phys.*, 62, 685–693, 2000.
- Forbes, J. M. and Zhang, X.: Quasi 2-day oscillation of the ionosphere: a statistical study, *J. Atmos. Sol. Terr. Phys.*, 59, 1025–1034, 1997.
- Laštovička, J.: Forcing of the ionosphere by waves from below, *J. Atmos. Sol. Terr. Phys.*, 68, 479–497, 2006.
- Mendillo, M., Rishbeth, H., Roble, R. G., and Wroten, J.: Modelling F2-layer seasonal trends and day-to-day variability driven by coupling with the lower atmosphere, *J. Atmos. Sol. Terr. Phys.*, 64, 1911–1931, 2002.
- Radicella, S. M.: Proceedings of the IRI Task Force Activity 2002, Report IC/IR/2003/3, Abdus Salam International Centre for Theoretical Physics, Trieste, 2003.
- Rishbeth, H.: Day-to-day ionospheric variations in a period of high solar activity, *J. Atmos. Sol. Terr. Phys.*, 55, 165–171, 1993.
- Rishbeth, H.: How the thermospheric circulation affects the ionospheric F2-layer, *J. Atmos. Sol. Terr. Phys.*, 60, 1385–1402, 1998.
- Rishbeth, H.: F-region links with the lower atmosphere?, *J. Atmos. Sol. Terr. Phys.*, 68, 469–478, 2006.
- Rishbeth, H. and Mendillo, M.: Patterns of F2-layer variability, *J. Atmos. Sol. Terr. Phys.*, 63, 1661–1680, 2001.
- Wilkinson, P. J.: Ionospheric variability and the international reference ionosphere, *Adv. Space Res.*, 34, 1853–1859, doi:10.1016/j.asr.2004.08.007, 2004.
- Zhang, S.-R. and Holt, J. M.: Empirically modeling ionospheric electron density variations using F107, E107 and MgII indices based on long-term incoherent scatter radar observations over Millstone Hill, Fourth (Virtual) Thermospheric/Ionospheric Geospheric Research (TIGER) Symposium, Internet, 10–14 June, 2002.

- Zhang, S.-R. and Holt, J. M.: Ionospheric plasma temperatures during 1976–2001 over Millstone Hill, *Adv. Space Res.*, 33, 963–969, doi:10.1016/j.asr.2003.07.012, 2004.
- Zhang, S.-R., Holt, J. M., Zalucha, A. M., and Amory-Mazaudier, C.: Mid-latitude ionospheric plasma temperature climatology and empirical model based on Saint Santin incoherent scatter radar data from 1966–1987, *J. Geophys. Res.*, 109, A11311, doi:10.1029/2004JA010709, 2004.
- Zhang, S.-R., Holt, J. M., van Eyken, A. P., McCready, M., Amory-Mazaudier, C., Fukao, S., and Sulzer, M.: Ionospheric local model and climatology from long-term databases of multiple incoherent scatter radars, *Geophys. Res. Lett.*, 32, L20102, doi:10.1029/2005GL023603, 2005.
- Zhang, S.-R. and Holt, J. M.: Ionospheric Climatology and Variability from Long-term and Multiple Incoherent Scatter Radar Observations: Climatology in Eastern American Sector, *J. Geophys. Res.*, 12, A06328, doi:10.1029/2006JA012206, 2007.